Synthetic Biology, 2017, 2(1): ysx007

doi: 10.1093/synbio/ysx007
Research article

Tailor-made exopolysaccharides—CRISPR-Cas9 mediated genome editing in *Paenibacillus polymyxa*

Marius Rütering[1,2], Brady F. Cress[2,3], Martin Schilling[4], Broder Rühmann[1], Mattheos A. G. Koffas[2,3], Volker Sieber[1,5,6], and Jochen Schmid[1,*]

[1]Chair of Chemistry of Biogenic Resources, Technical University of Munich, Straubing, Germany, [2]Center for Biotechnology and Interdisciplinary Studies, Rensselaer Polytechnic Institute, Troy, NY, USA, [3]Department of Chemical and Biological Engineering, Rensselaer Polytechnic Institute, Troy, NY, USA, [4]Evonik Nutrition and Care GmbH, Kirschenallee, Darmstadt, Germany, [5]Fraunhofer IGB, Straubing Branch Bio, Electro, and Chemocatalysis BioCat, Straubing, Germany and [6]Catalysis Research Center, Technical University of Munich, Garching, Germany

*Corresponding author: E-mail: j.schmid@tum.de

Abstract

Application of state-of-the-art genome editing tools like CRISPR-Cas9 drastically increase the number of undomesticated micro-organisms amenable to highly efficient and rapid genetic engineering. Adaptation of these tools to new bacterial families can open up entirely new possibilities for these organisms to accelerate as biotechnologically relevant microbial factories, also making new products economically competitive. Here, we report the implementation of a CRISPR-Cas9 based vector system in *Paenibacillus polymyxa*, enabling fast and reliable genome editing in this host. Homology directed repair allows for highly efficient deletions of single genes and large regions as well as insertions. We used the system to investigate the yet undescribed biosynthesis machinery for exopolysaccharide (EPS) production in *P. polymyxa* DSM 365, enabling assignment of putative roles to several genes involved in EPS biosynthesis. Using this simple gene deletion strategy, we generated EPS variants that differ from the wild-type polymer not only in terms of monomer composition, but also in terms of their rheological behavior. The developed CRISPR-Cas9 mediated engineering approach will significantly contribute to the understanding and utilization of socially and economically relevant *Paenibacillus* species and extend the polymer portfolio.

Key words: exopolysaccharides; CRISPR-Cas9; genome editing; *Paenibacillus polymyxa*

1. Introduction

Value-added compounds synthesized by microorganisms, such as alkaloids, flavonoids, terpenoids, polyketides, lipopeptides, biofuels and exopolysaccharides (EPSs), are of huge interest for a variety of applications in the food, medicine, agriculture and consumer goods industries (1–3). Although advances in synthetic biology and metabolic engineering have significantly contributed to the design of improved microbial factories, robust heterologous expression of complex pathways is often hampered by product toxicity, low yields and the absence or insufficient availability of biosynthetic precursors (4, 5). State-of-the-art genome editing tools like CRISPR-Cas9 rapidly increase the accessibility of undomesticated strains to genetic engineering, and therefore pave the way for taming wild-type (WT) species in order to construct new, biotechnologically relevant production strains (6). Thorough implementation of such tools in a species of interest is of fundamental importance for efficient rewiring of metabolic circuits and optimization or alteration of the produced

Submitted: 26 August 2017; **Received (in revised form):** 24 October 2017. **Accepted:** 16 November 2017

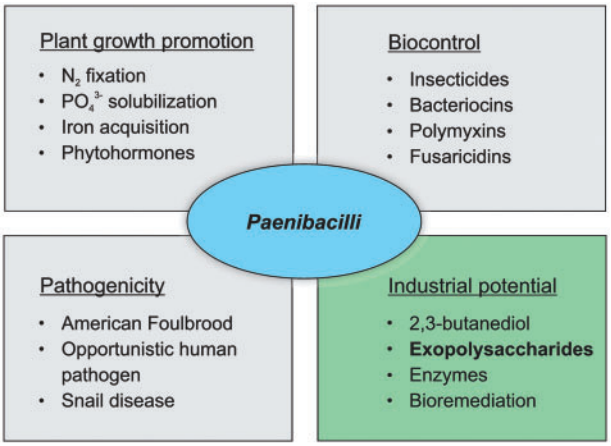

Figure 1. Relevance of *Paenibacilli* for agriculture, society and industry. The main subject of this study, exopolysaccharides, are highlighted. A detailed review on all aspects can be found in reference (36).

metabolites. Gram-positive bacteria of the phylum firmicutes are promising candidates for this endeavor. Their robustness toward environmental stress in combination with their promiscuity toward different carbon sources, the huge variety in gene clusters dedicated to secondary metabolite production and their well-established cultivatibility exemplify their potential as customizable microbial factories (7–11). Several genera of this phylum, like *Lactobacillus* and *Clostridium*, have been used in biotechnology for centuries, both consciously and unconsciously (12,13). Numerous recent studies demonstrated the successful application of CRISPR-Cas9 in a variety of firmicute families including *Bacillaceae*, *Lactobacillaceae*, *Clostridiaceae* and *Staphylococcaceae* (14–19). However, no reports on CRISPR-Cas9 based genome editing tools for *Paenibacillaceae* are available yet, and existing genetic engineering approaches are limited due to low efficiencies or the dependence on integration of selectable markers (20,21). Nevertheless, this family comprises several species of economic and social relevance (Figure 1). *Paenibacillus larvae*, for example, is the causative agent of American Foulbrood, a lethal disease of honeybee larvae (22), posing grave concern for the future of agriculture, and some *Paenibacilli* are known to be opportunistic human pathogens (23,24). Easily deployable vectors facilitating rapid elucidation of the genetic basis for pathogenicity, immunogenicity and toxicity would hold tremendous scientific value. On the constructive side, numerous studies describe the beneficial use of *Paenibacilli* in miscellaneous fields. In agriculture, they are critical because of their intrinsic capacity for nitrogen fixation (25) and phosphate solubilization (26), thereby directly promoting plant growth. Furthermore, they produce a variety of insecticides (27) and antimicrobials like polymyxins (28) and fusaricidins (29), which protect plants from phytopathogens and have potential use in medical applications. Their extensive enzymatic capabilities to degrade complex carbohydrates and to produce and tolerate high levels of commercially relevant chemicals like 2,3-butanediol, for example, make *Paenibacilli* an interesting genus for the fermentative production of this and other platform chemicals from renewable resources (30). Critically, they produce a class of still underappreciated but highly promising EPSs possessing antioxidant activity and outstanding rheological properties, qualifying them for applications in therapeutics or as thickeners (31–35). Grady *et al.* (36) recently reviewed the potential of *Paenibacilli* in agriculture and industrial biotechnology in detail.

EPSs are linear or branched, high-molecular weight polymers composed of sugars molecules, which are secreted into the extracellular environment during microbial growth. Due to variations in monomer composition, molecular weight and decoration with functional groups, these polymers exhibit an immense physicochemical versatility making them interesting for various applications (37). This structural variability is highlighted by the existence of over 350 annotated EPSs from prokaryotes (38). EPSs have been primarily used as rheological additives for food, agricultural feed, oil recovery and cosmetic applications (39). Prominent representatives of commercialized EPSs are sphinganes, xanthan, pullulan, dextran and levan (40–42). Although these compounds hold big shares of the markets for bio-based viscosifiers and gelling agents, they are only narrowly suited for specialized applications matching their imparted rheologies. Especially high-value niche applications like tissue engineering, cell encapsulation or drug delivery require explicitly defined physicochemical characteristics, which are not covered by the existing EPSs (43) without further, post-biosynthetic chemical or enzymatic modification.

Using synthetic biology for design and synthesis of tailor-made EPSs is a highly promising approach to fill these gaps. The aforementioned structural diversity of existing EPSs makes their associate biosynthetic pathways ideal templates for generating polymers with tunable properties through the rational engineering of novel structures (44). Typical targets for EPS engineering are functional groups like pyruvyl groups, which contribute to polymer charge density and thereby influence the rheological traits (45). However, the adjustment of substituent patterns only allows for alterations in the degree of superficial decorations while leaving the core, underlying glycan structure and sequence unchanged. Other engineering targets are the glycosyltransferases (GTs), which transfer defined sugar moieties to the nascent, pre-assembled repeating units and thereby determine the composition and linkage pattern of the mature EPS (46,47). Complementation experiments have shown that exchange of GTs with distinct monosaccharide preferences is feasible, indicating that the EPS polymerization and secretion machinery of one organism can potentially be harnessed for the production of various polymers with disparate structures and properties (37). The combination of in-depth characterizations of known and to-be-discovered GTs with protein-engineering will eventually yield a catalog of enzymes, which can be used for the directed incorporation of user-specified sugars imparting desired properties (48). Polymer variants produced in this fashion will successively contribute to the still superficial understanding of EPS structure–function relationships and thereby ultimately allow for the rational design of application-defined properties (43). Modern synthetic biology tools, such as CRISPR-Cas9, will not only facilitate engineering of structural features but will also drastically accelerate strain improvements, spurring the rise of robust and economical production processes for competitive, custom-made EPSs.

In this study, we describe the development of a CRISPR-Cas9 based genome-editing tool for *Paenibacillus polymyxa*. The single plasmid system was employed for highly efficient, homology directed deletions as well as integrations. The developed CRISPR method was subsequently used to annotate and provide the first experimental evidence of the gene cluster responsible for EPS biosynthesis in *P. polymyxa* DSM 365. Besides shutting down and significantly attenuating EPS biosynthesis, we were also able to produce structurally altered EPSs exhibiting fundamentally distinct rheological properties. On the basis of these findings, putative substrate specificities of two GTs were assigned.

We envision that this system will be used to further decipher and harness the EPS biosynthesis machinery of *P. polymyxa* in order to construct a generic host, capable of producing polymers with disparate structures. Furthermore, the CRISPR method developed here should expedite investigation of several other important fields related to *Paenibacilli*, including production of value-added chemicals or answering fundamental questions about host–pathogen interactions for socially important diseases caused by *Paenibacilli*, like the American Foulbrood.

2. Materials and methods

2.1 Plasmids, bacterial strains, primers and growth conditions

The bacterial strains, plasmids and oligonucleotides used in this study are listed in Supplementary Tables S1–S3. *Escherichia coli* strains were grown in Lysogen-broth (LB; 10 $g \cdot l^{-1}$ sodium chloride, 10 $g \cdot l^{-1}$ peptone and 5 $g \cdot l^{-1}$ yeast extract) at 37 °C. *Paenibacillus polymyxa* DSM365 (DSMZ, Braunschweig, Germany) was cultured at 30 °C in LB for genetic manipulations and in MM1 P100 for EPS production and phenotype evaluations [30 $g \cdot l^{-1}$ glucose, 1.33 $g \cdot l^{-1}$ magnesium sulfate heptahydrate, 1.67 $g \cdot l^{-1}$ potassium dihydrogen phosphate, 0.05 $g \cdot l^{-1}$ calcium chloride dihydrate, 2 $ml \cdot l^{-1}$ RPMI 1640 vitamins solution (Sigma-Aldrich) and 1 $ml \cdot l^{-1}$ trace elements solution containing 2.5 $g \cdot l^{-1}$ iron (II) sulfate heptahydrate, 2.1 $g \cdot l^{-1}$ sodium tartrate dihydrate, 1.8 $g \cdot l^{-1}$ manganese (II) chloride tetrahydrate, 0.075 $g \cdot l^{-1}$ cobalt (II) chloride hexahydrate, 0.031 $g \cdot l^{-1}$ copper (II) sulfate heptahydrate, 0.258 $g \cdot l^{-1}$ boric acid, 0.023 $g \cdot l^{-1}$ sodium molybdate and 0.021 $g \cdot l^{-1}$ zinc chloride] (32). Antibiotics were added at 50 $\mu g \cdot ml^{-1}$ for neomycin and 20 $\mu g \cdot ml^{-1}$ for polymyxin.

2.2 Construction of pCasPP

For construction of the pCasPP plasmid, the Cas9 gene was amplified alongside with the BbsI flanked lacZ cassette from pCRISPRomyces-2, which was a gift from Huimin Zhao (Addgene plasmid # 61737). The neomycin resistance and the repU gene were amplified from pUBoriMCS, which is a pUB110 derivate (49), containing a BbsI inserted origin of replication as well as a multiple cloning site from pUC18. A BsaI site within repU was removed by introducing a silent mutation with the utilized primers. The sgsE promotor (50) was obtained as artificial gBlock (Integrated DNA Technologies). A cytosine was replaced by a guanine to delete an interfering BbsI site. All five fragments were assembled via Golden Gate using BsaI. The oriT was amplified from pCRISPRomyces-2 and cloned into a XbaI restriction site afterwards. Subsequently, the unique SpeI site was added by introducing the desired sequence mutations while PCR-amplifying the pCasPP plasmid in two pieces with corresponding primers. To inactivate Cas9, the same procedure was deployed and the two active sites were mutated to D10A and H840A, yielding pdCasPP. All cloning and mutation steps were verified by sequencing (Eurofins, Ebersberg, Germany).

2.3 Bioinformatics

In order to identify genes involved in EPS biosynthesis, the *P. polymyxa* DSM 365 genome was uploaded to RAST for automated genome annotation (51). Obtained data was screened manually and putatively identified genes involved in EPS-biosynthesis were annotated in detail using NCBI blastx (52) and UniProt blast (53). Intracellular protein localizations were predicted using CELLO v.2.5 (54). Biosynthetic pathways involved in nucleotide sugar production were identified using KEGG (55). Twenty base pair long spacers for Cas9 mediated edits were selected based on on- and off-target scores determined with benchling (http://www.benchling.com) using NGG as PAM motif and the uploaded *P. polymyxa* DSM 365 genome as reference. *In silico* cloning and sequence alignments were performed with SnapGene software (GSL Biotech, Chicago, IL, USA).

2.4 Genome editing in *Paenibacillus polymyxa* DSM 365

CRISPR-Cas9 mediated genome editing in *P. polymyxa* DSM 365 was performed as follows. Subsequent to spacer selection using benchling (http://www.benchling.com), 24 bp oligos for guide annealing were designed as described in the supplemental material of Cobb *et al.* (56). Oligonucleotides were phosphorylated, annealed and finally inserted into the pCasPP backbone via Golden Gate assembly. Subsequent to guide cloning, homologous regions were constructed by overlap extension PCR and inserted by restriction and ligation into the SpeI site. A detailed description of the entire cloning procedure can be found in the supplementary information. Constructed plasmids were sequenced and then transferred to *E. coli* S17-1 for conjugation events. Plasmid transfer from *E. coli* S17-1 to *P. polymyxa* DSM 365 was performed as follows. Overnight cultures of recipient and donor strains were subcultured 1:100 in non-selective or selective LB media, respectively, and grown until early exponential phase (4 h). Afterwards, 900 µl of the recipient culture were heat shocked for 15 min at 42 °C and mixed with 300 µl of the donor strain culture. Cells were harvested by centrifugation for 3 min at 8000 × g and the pellet was gently resuspended and dropped on non-selective LB agar. After overnight incubation at 30 °C, cells were scraped from the agar, resuspended in 500 µl 0.9% NaCl and plated on LB agar containing neomycin and polymyxin for counter selection. *Paenibacillus polymyxa* conjugants were obtained after 48 h incubation at 30 °C and screened for editing events using colony PCR. Sequence verification of genome edits was performed by amplifying edited regions from isolated genomic *P. polymyxa* DNA using suitable primers. Obtained PCR products were purified, adjusted to a concentration of 10 $ng \cdot \mu l^{-1}$, mixed with corresponding primers, and sent for sequencing.

2.5 EPS production and purification

For polymer production, baffled 250 ml shake flasks sealed with aluminum caps were filled with 100 ml MM1 P100 media and inoculated with 1 ml of a *P. polymyxa* overnight culture. Cultures were incubated at 30 °C and 170 rpm for 28 h. To extract EPS from shake-flask experiments, the culture broth was diluted 1:3 with distilled water to decrease viscosity and centrifuged for 30 min at 17 600 × g and 20 °C to separate cells. Subsequently, EPS was precipitated by slowly pouring the supernatant into two volumes of 2-propanol. The precipitated polymer was collected using a spatula and dried overnight at 45 °C in a VDL 53 vacuum drying oven (Binder, Tuttlingen, Germany).

2.6 Molecular weight determinations

Gel permeation chromatography was performed using an Agilent 1260 Infinity system (Agilent Technologies, Waldbronn, Germany) equipped with a refractive index detector and a SECurity SLD7000 7-angle static light-scattering detector (PSS Polymer Standards Service GmbH, Mainz, Germany). Samples were analyzed using a Suprema guard column, one Suprema 100 Å (8 × 300 mm) and two

Suprema 10 000 Å (8 × 300 mm) columns (PSS Polymer Standards Service). The eluent, 0.1 M $LiNO_3$, was pumped at a flow rate of 1 ml·min^{-1} and the column compartment was kept at 50 °C. Samples were injected in 60 min intervals. Qualitative molecular weight results were obtained by comparing sample elution profiles with a 12-point pullulan standard curve.

2.7 Carbohydrate fingerprint

Simultaneous high resolution detection of carbohydrates which can be derivatized with 1-phenyl-3-methyl-5-pyrazolone (PMP) was performed via HT-PMP as described before (57). Briefly, 1 g·l^{-1} solutions of EPS were hydrolyzed in 2 M trifluoroacetic acid (TFA) for 90 min at 121 °C and subsequently neutralized with 3.2% (v/v) ammonium hydroxide. Thereafter, 25 µl neutralized sample were mixed with 75 µl derivatization reagent (0.1 M methanolic-PMP-solution:0.4% ammonium hydroxide solution 2:1) and incubated for 100 min at 70 °C. Finally, 130 µl of 19.23 mM acetic acid were added to 20 µl cooled sample and HPLC separation was performed on a reverse phase column (Gravity C18, 100 mm length, 2 mm i.d.; 1.8 µm particle size; Macherey-Nagel) tempered to 50 °C. For gradient elution, mobile phase A [5 mM ammonium acetate buffer (pH 5.6) with 15% acetonitrile] and mobile phase B (pure acetonitrile) were pumped at a flow rate of 0.6 ml·min^{-1}. The HPLC system (Ultimate 3000RS, Dionex) was composed of a degasser (SRD 3400), a pump module (HPG 3400RS) auto sampler (WPS 3000TRS), a column compartment (TCC3000RS), a diode array detector (DAD 3000RS) and an ESI-ion-trap unit (HCT, Bruker). Standards for each sugar (2, 3, 4, 5, 10, 20, 30, 40, 50 and 200 mg·l^{-1}) were processed as the samples, starting with the derivatization step. Data were collected and analyzed with BrukerHystar, QuantAnalysis and Dionex Chromelion software.

2.8 Pyruvate assay

To determine the pyruvate content of the polymers, 1 g·l^{-1} EPS solutions were hydrolyzed and neutralized as described for the sugar monomer analyses (58). To start the reaction, 10 µl neutralized sample + 90 µl of ddH_2O or standard were mixed with 100 µl assay mixture [50 µM N-(carboxymethylamino-carbonyl)-4.4′-bis(dimethylamino)-diphenylamine sodium salt (DA-64), 50 µM thiamine pyrophosphate, 100 µM $MgCl_2 \times 6H_2O$, 0.05 U·ml^{-1} pyruvate oxidase, 0.2 U·ml^{-1} horseradish peroxidase, 20 mM K_2PO_4 buffer pH 6] and incubated at 37 °C, 700 rpm for 30 min in a micro-plate shaker. The extinction was measured at 727 nm and subtracted with values measured at 540 nm to eliminate background signals. Nine standards in the range from 0.5 to 100 µM pyruvate were used for calibration.

2.9 Rheological measurements

Rheological measurements were performed with an air-bearing MCR300 controlled-stress rheometer (Anton Paar Germany GmbH) using a cone plate geometry (50 mm diameter, 1° cone angle, 0.05 mm gap) at a constant, Peltier-controlled temperature of 20 °C. Data was collected and analyzed with Rheoplus V.3.61 software (Anton Paar). Viscosity curves were obtained during a logarithmic shear-rate ramp ($\dot{\gamma} = 0.1$–$1000\,s^{-1}$). The linear viscoelastic range and further structural features of polymer solutions were determined with a shear stress amplitude sweep from 0.1 to 1000 Pa at a constant frequency of $f = 1$ Hz. Time dependent flow behavior at non-destructive stress was assessed during frequency sweeps from 0.01 to 100 Hz. All measurements were carried out in triplicates.

3. Results and discussion

3.1 CRISPR-Cas9 vector system

Design and construction of the pCasPP CRISPR-Cas9 expression plasmid (Figure 2) was inspired by a vector system which was efficiently used for genome editing in *Streptomyces* (56). *Streptococcus pyogenes* Cas9 (SpCas9) and synthetic guide RNA (sgRNA) region, including the BbsI flanked lacZ selection cassette and origin of transfer (oriT), were amplified from pCRISPomyces-2 plasmid. The Cas9-encoding gene was set under transcriptional control of the broad-host-range S-layer gene promoter sgsE from *Geobacillus stearothermophilus*, which was previously shown to be functional in *Paenibacillus alvei* (21,50). Since the transcription start for guide expression is crucial for guide length and thereby targeting efficiency, the constitutive *gapdh* promoter for sgRNA expression was not changed. To the best of our knowledge, this is the first report on *gapdh* promoter functionality in *Paenibacilli*. Origin of replication (ori), neomycin resistance gene and the *repU* gene, involved in plasmid replication (59), were amplified from pUBori, a pUB110-derived plasmid which is readily taken up and propagated by *P. polymyxa* (unpublished data). All DNA parts were assembled using Golden Gate cloning (60). A unique SpeI site was utilized for insertion of homologous arms (1 kb upstream and 1 kb downstream, fused by overlap extension PCR), necessary for homology directed repair (HDR) after successful double strand break by the activity of Cas9.

Insertion of 20 bp long single guide spacers was performed via BbsI based Golden Gate cloning of annealed and phosphorylated primers. For multiplexing, gBlocks comprising two copies of the sgRNA region were utilized as described for the pCRISPRomyces-2 system (56). Plasmid transfer to *P. polymyxa* DSM 365 was conducted via conjugation using the *E. coli* S17-1 donor strain and counter-selection on polymyxin-containing media. The functionality of the designed system was first tested on a putative glycosyltransferase (*pepF*) of the hypothetical EPS cluster. Using this target, different variants of the pCasPP plasmid were assembled, and transformation efficiencies were evaluated (Table 1, Supplementary Figure S1).

Guided Cas9 resulted in high lethality in the absence of a repair template, yielding less than 0.2% colonies compared to the dummy plasmid pCasPP. Although not examined further, it is likely that these colonies resulted from escape mutation as reported by others (61). When a HDR template was included, the survival rate increased significantly, and >200 clones were obtained, independently of the chosen spacer. A plasmid containing a non-targeting gRNA and homologous arms resulted in less conjugants than the dummy, which is probably due to reduced conjugation efficiency of the larger vector, but in noticeably more colonies than the guided variants. Colony PCR confirmed that all tested colonies transformed with the guided plasmid containing a repair template were successful knockout events (eight individual conjugants), whereas tested colonies from all other plasmid transformations showed to be the unedited WT (Supplementary Figure S2). Sequencing of at least three clones from pCasPP, pCasPP-pepFsg1 and pCasPP-pepFsg1-harms corroborated this finding. These results suggest that the non-homologous end-joining (NHEJ) DNA repair based on the Ku and LigD enzymes is not functional or insufficient to introduce indels in *P. polymyxa*, although the required genes for NHEJ are encoded within the organism's genome (62). To more

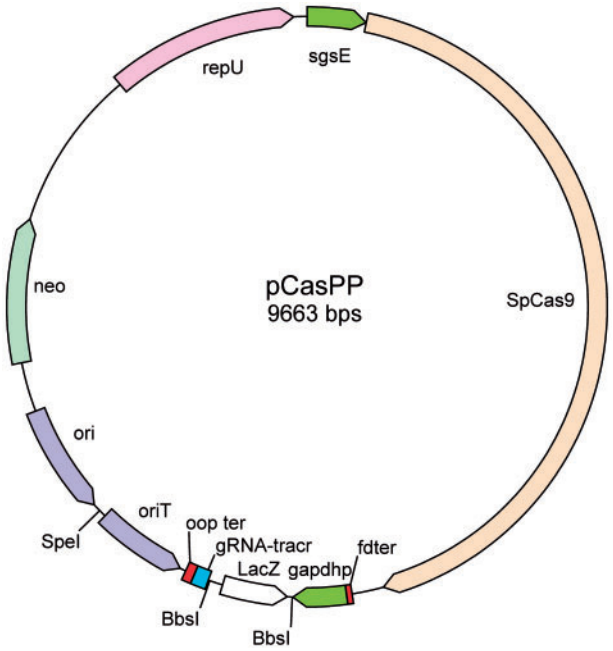

Figure 2. CRISPR-Cas9 vector system. Promoter sgsE controls SpCas9 expression, gapdh promoter regulates guide RNA levels. Spacer insertion is performed via Golden gate using BbsI. The unique SpeI site allows for insertion of homologous regions for HDR.

Table 1. Conjugation efficiency of different pCasPP derivatives

Plasmid	Colonies/ conjugation	Description
pCasPP	>10 000	Non-targeting plasmid; no repair template
pCasPP-pepFsg1	<20	Targeting *pepF* at Site 1; no repair template
pCasPP-pepFsg1-harms	>200	Targeting *pepF* at Site 1; repair template provided
pCasPP-pepFsg2-harms	>200	Targeting *pepF* at Site 2; repair template provided
pCasPP-harms	>1000	Non-targeting plasmid; repair template provided

thoroughly assess the efficiency of the system, another knockout (Δ*ugdH1*, found to result in phenotypically distinguishable colonies as a consequence of reduced EPS production) was investigated. Due to the ease of screening this knockout by colony morphology, a much larger sample of 50 colonies for each of two distinct spacers within the *ugdH1* ORF were analyzed for their phenotypic appearance. Edited conjugants appeared as irregular, flat, opaque colonies with a brittle, dry consistency. WT colonies in contrast were loosely attached, circular and convex with a highly mucoid consistency. All conjugants for both spacers showed the phenotype consistent with an edited strain (Supplementary Figure S3). For all other edits described in this study, at least eight isolated colonies were analyzed using colony PCR, and each successful knockout was verified via sequencing.

In order to perform deletions in series, it is critical that the CRISPR-Cas9 plasmid is curable, so that the vector can be recursively transformed with new sgRNA inserts. Toward this end, we found that curing of the plasmid after editing was readily achieved by incubating liquid cultures of the knockout mutant for 72 h at elevated temperatures (37 °C) in absence of antibiotic with a single 1:100 sub-culturing after 36 h. Curing efficiency was assessed for the WT strain and six knockout strains. Specifically, eight colonies obtained from a culture of each knockout strain (by plating dilution series on non-selective agar) were picked and streaked on neomycin plates to test for neomycin sensitivity and to thus determine the curing efficiency. Out of the eight colonies obtained from subculture of each knockout strain, a cured colony sensitive to neomycin was readily found in each case (typically approximately 75% of tested colonies), confirming that the vector can be cured easily (Supplementary Figure S4). To investigate the possibility of performing genome-integration of heterologous DNA with the constructed system, a 300 bp *pgrac* promoter region was cloned between the 1 kb homologous regions of *sacB*, a gene encoding for a levansucrase in the *P. polymyxa* genome, and the editing experiments were performed as described above. All eight tested clones were colony PCR positive and sequencing verified the successful integration of the artificial *pgrac* promoter sequence, proving the functionality of pCasPP for genome integration (Supplementary Figure S5).

3.2 Exopolysaccharide biosynthesis in *Paenibacillus polymyxa* DSM 365

Fundamental mechanisms of polysaccharide synthesis in bacteria have been extensively investigated in organisms such as *E. coli*, *X. campestris* and *S. pneumoniae* (63–65). While research on polysaccharide gene clusters in Gram-negatives started as early as the 1980 s, the first studies on EPS genetics in Gram-positive bacteria were published approximately 20 years later (66). The best-characterized clusters of Gram-positive representatives are those of *Lactobacillaceae* and *Streptococcoaceae*. EPS production by *Paenibacillacae* is also described by several reports (34). However, except for the levansucrase catalyzed production of levan in the presence of sucrose as carbon source (67), the genetic basis for the biosynthesis of heteropolysaccharides in this genus is unknown territory. To use the implemented genome editing tool for elucidation and engineering of EPS synthesis, the published *P. polymyxa* DSM 365 genome (62) was mined, and putative EPS-related genes were annotated thoroughly (accession number: BK010330).

The majority of coding sequences putatively involved in EPS synthesis were found clustered together, as is typical for most heteropolysaccharides (37) (Figure 3, Table 2).

The size of the locus is at the high end of known bacterial EPS gene clusters, spanning almost 35 kb and comprising 28 coding sequences that could be assigned to polysaccharide production or hydrolysis. EPS gene clusters from *Lactobacilli* typically comprise 14 to 18 kb (68,69), whereas clusters from *S. thermophilus* can be up to 35 kb in size (70). Interestingly, several functional elements within the *P. polymyxa* DSM 365 EPS-cluster appear to be encoded twice. This could indicate an evolutionary development of the strains towards reliable EPS production. Another explanation could be that the strain is capable of producing two different polymers, with some genes being involved in both pathways (e.g. polymerases and precursors) and some being unique for each polymer (GTs). Some genes associated with precursor supply are encoded one (*ugdH*) or two more times (*manC*, *galU*) at different loci of the genome. *Fcl* and *gmd* are exclusively found within the cluster.

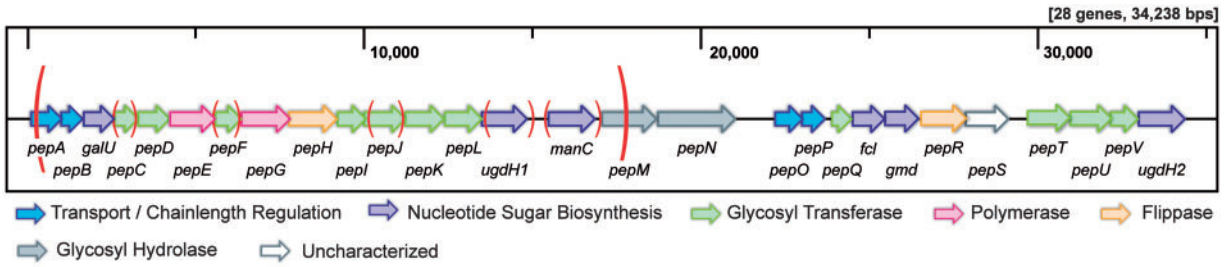

Figure 3. Gene cluster of *P. polymyxa* DSM 365 encoding for exopolysaccharide biosynthesis (accession number: BK010330). Blue arrows represent genes that are putatively involved in chain length determination. Purple arrows represent genes responsible for nucleotide sugar synthesis, pink arrows stand for genes, which encode membrane-spanning polymerases, light green arrows show genes that are annotated glycosyl transferases and orange arrows represent genes encoding flippases. Grey arrows represent genes encoding glycosyl hydrolases. The regions highlighted with red brackets were deleted during knockout experiments.

Table 2. Hypothetical annotation of clustered genes involved in exopolysaccharide biosynthesis

Gene	Length [aa]	Localization[a]	Protein family[b]	Function[b]	Accession number
pepA	302	Membrane	Wzz	Chain length determination	E0RL99
pepB	212	Cytoplasmic, membrane	Wzc	Regulation	A0A074M2H7
galU	300	Cytoplasmic	galU	Precursor	E0RLA1
pepC	232	Cytoplasmic	GT	Priming transferase[c]	E0RLA2
pepD	311	Cytoplasmic	GT2	Transferase, assembly	A0A074LI20
pepE	445	Membrane	Wzy_C	Polymerase	A0A074LD40
pepF	256	Cytoplasmic	WecB (GT26)	Galactosyltransferase[c], assembly	E0RLA5
pepG	480	Membrane	Wzy_C	Polymerisation	A0A074LK02
pepH	472	Membrane	Wzx	Flippase	A0A074LG88
pepI	279	Cytoplasmic	GT2	Transferase, assembly	A0A074LI22
pepJ	407	Cytoplasmic	GT4	Mannosyltransferase[c], assembly	A0A074LD42
pepK	382	Cytoplasmic	GT1	Transferase, assembly	A0A074M2I1
pepL	366	Cytoplasmic	GT4	Transferase, assembly	A0A074LK07
ugdH1	445	Cytoplasmic	UDPG_MGDP_dh	Precursor	A0A074LG92
manC	458	Cytoplasmic	PMI	Precursor	E0RLB3
pepM	535	Extracellular	GH26	Hydrolysis	A0A074LD47
pepN	765	Extracellular	Glycoside_hydrolase_SF	Hydrolysis	A0A074M2I4
pepO	270	Membrane	Wzz	Chain length determination	E0RLB8
pepP	228	Membrane	Wzc	Regulation	A0A074LD53
pepQ	192	Membrane	GT	Priming transferase[c]	E0RLC0
fcl	312	Cytoplasmic	Epimerase	GDP-fucose-synthase	A0A074LK14
gmd	329	Cytoplasmic	gmd	Precursor	E0RLC2
pepR	447	Membrane	Wzx	Flippase	A0A074LI33
pepS	420	Cytoplasmic	uncharacterized	unknown	A0A074LD55
pepT	416	Cytoplasmic	GT1	Transferase, assembly	A0A074M2J0
pepU	405	Cytoplasmic	GT1	Transferase, assembly	A0A074LK16
pepV	269	Cytoplasmic	WecB (GT26)	Transferase, assembly	A0A074LGA5
ugdH2	456	Cytoplasmic	UDPG_MGDP_dh	Precursor	E0RLC8

Uncharacterized genes were named alphabetically from *pepA* though *pepV*. Confidently annotated enzymes involved in nucleotide sugar synthesis are named according to standards used in literature.

[a]Protein localizations were predicted using CELLO v.2.5.

[b]Family and putative function assignment is based on domain comparisons in the Pfam database.

[c]Putative function assignment based on results obtained in this study.

The encoded proteins suggest that EPS assembly and secretion in *P. polymyxa* follows the Wzx/Wzy dependent pathway, which is common in Gram-positive and Gram-negative bacteria and is also utilized for EPS formation in *Lactococci* and *Streptococci* (64). Through this pathway, the repeating units of the polymer are assembled on the inner side of the cytoplasmic membrane by GTs, starting with the transfer of the first sugar to a membrane bound lipid undecaprenyl carrier via the so-called priming GT. Thereafter, the nascent polysaccharide repeating unit is elongated through successive addition of distinct sugars by the other GTs. The fully assembled repeating units are then transferred over the membrane by a Wzx flippase and finally polymerized by the Wzy protein in reducing-end growth via a block transfer mechanism. A schematic representation of the hypothetical Wzx/Wzy dependent biosynthesis machinery of *P. polymyxa* is presented in Figure 4.

3.3 Exopolysaccharide engineering

The ultimate objective of the presented EPS engineering approach was to alter the chemical structure of the produced EPS in order to influence the physicochemical characteristics of the secreted polymer, yielding EPSs with new or superior material properties.

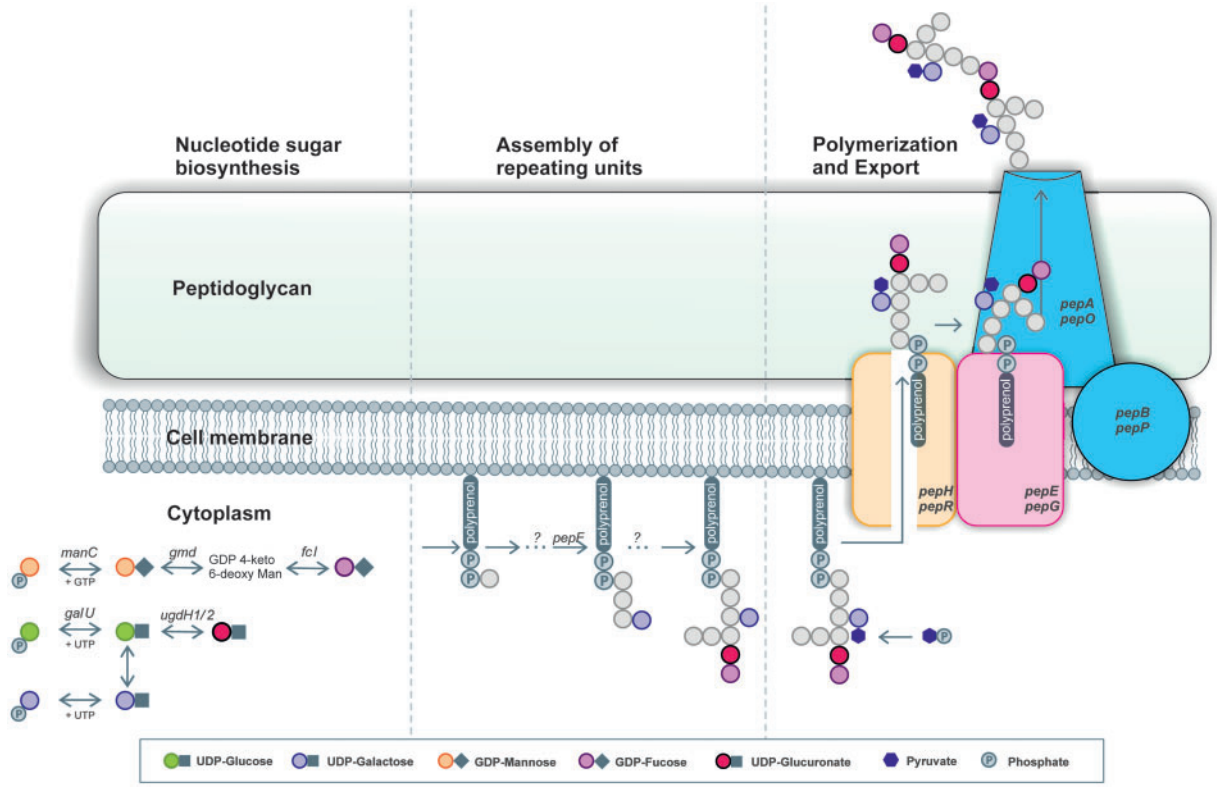

Figure 4. Schematic overview of the putative EPS biosynthesis machinery of *P. polymyxa*. Labeled proteins are encoded in the described gene cluster. Synthesis and interconversion of the different precursors occurs in the cytoplasm. Activated nucleotide sugars are then transferred to the membrane anchored lipid carrier by glycosyl transferases. Colored sugar monomers of the repeating unit are annotations as concluded from mass spectrometry analyses. After assembly, repeating units are transported across the membrane by a flippase (encoded by *pepH* and *pepR*) and then polymerized by Wzy (encoded by *pepE* and *pepG*). Chain length determination is probably controlled by Wzz (*pepA* and *pepO*) and Wzc (encoded by *pepB* and *pepP*) analogs.

To achieve this goal, the developed CRISPR-Cas9 system was deployed for gene disruption studies targeting different genes within the identified EPS cluster. Five different genes were deleted individually, three of which are putative GTs (*pepF*, *pepJ*, *pepC*), and two of which are probably involved in precursor synthesis (*ugdH1*, *manC*). Additionally, an 18 kb fragment was deleted (*clu*), to generate an EPS deficient mutant (Figure 5). Details on the deletion sites can be found in Supplementary Table S4. After successful verification of deletions, strains were cured of the plasmid, and EPS of each mutant and WT strain was produced and purified under standardized conditions in biological triplicates (Table 3). To prevent falsification of EPS data by levan production, the utilized fermentation media contained glucose as sole carbon source. In a previous study, we showed that this media composition results in heteropolysaccharide production only (31).

All mutant strains produced less EPS than the WT, with Δ*pepF* and Δ*pepJ* still producing relatively high quantities, Δ*pepC* and Δ*ugdH1* secreting considerably less and with Δ*manC* and Δ*clu* not producing any precipitable polymer. Diminished EPS titers after deletions of GTs are in accordance with studies in *Lactobacilli*, *Xanthomonas* and *Streptococci* reporting similar effects upon inactivation of transferases (71–73). In particular, priming GTs are known to be essential for EPS formation, resulting in EPS deficient mutants if deleted. The importance of enzymes involved in biosynthesis of nucleotide sugars is also described in literature. It has been shown many times that levels of key intermediates for nucleotide sugar biosynthesis directly correlate with obtained EPS titers (74). Li *et al.* (75) described the crucial role of two UDP-xylose synthases (*uxs*) for EPS formation in a related *Paenibacillus* strain, secreting a xylose containing EPS. Inactivation of the first *uxs* gene reduced EPS titers by 50% and deletion of the second copy abrogated EPS biosynthesis completely. By disruption of the 18 kb fragment (Δ*clu*) in *P. polymyxa*, all genes involved in polymerization (*pepE*, *pepG*) of the glycan were removed, logically resulting in an EPS deficient mutant. Knockout of *manC* creates a mutant that is not capable of producing GDP-Mannose and GDP-Fucose (Figure 6). At least one of these nucleotide sugars is probably an essential building block of the repeating unit, because deletion results in non-polymerizable or non-precipitable carbohydrates.

To characterize the EPSs produced by the *P. polymyxa* mutants and WT strain, molecular weights and monomer compositions of obtained polymers were analyzed. Molecular weights of all polymers were found to be in the same range (Table 3) and comparable to values found for *Paenibacillus* heteropolysaccharides in literature (76).

Of note, the Δ*manC* mutant still showed a small but non-negligible polymer peak in GPC analyses, which was in the same order of magnitude in MW as all other polymers, indicating that still some full-length polymer was formed, but too little to allow for processing (Supplementary Figure S6). A possible explanation for this observation is that basal expression of the two other *manC* copies encoded in the genome compensates the deletion to a very little extent. Since regulation of cluster expression is presumably decoupled from the regulation of the other *manC* versions, this compensation is only marginal.

Similar findings were reported for capsule biogenesis in *Streptococci* (77). No polymer peak was observable by GPC for the Δ*clu* mutant, experimentally proving that EPS biosynthesis was eliminated.

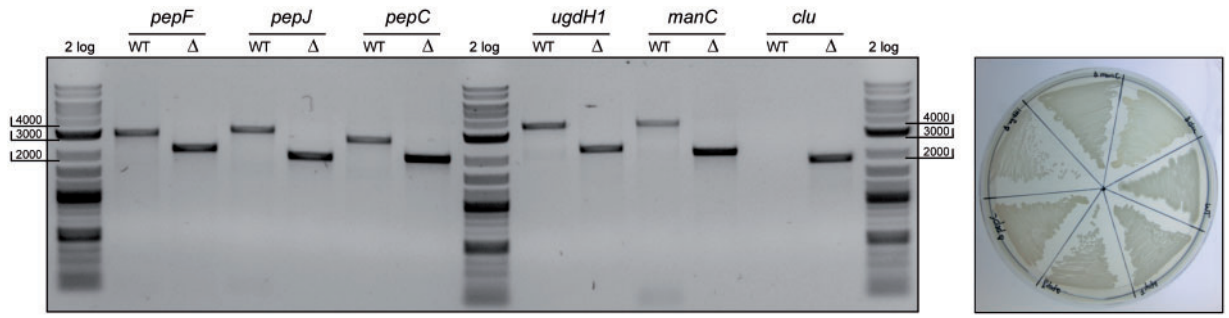

Figure 5. CRISPR-Cas9 mediated knockout studies in *P. polymyxa*. The agarose gel shows PCR analyses from purified genomic DNA of WT and knockout mutants (Δ) for each target. Repair templates were provided by fusing 1 kb upstream and 1 kb downstream regions of the gene of interest, and PCR amplification of this region in the modified strain resulted in an ∼2 kb band, indicating successful disruptions. The WT PCR for the 18 kb fragment (*clu*) does not yield a PCR product with the chosen polymerase due its large size. Phenotype analysis of the generated mutants revealed that all strains were viable under standard growth conditions.

Table 3. Data on EPSs produced by the WT strain and the generated deletion mutants

Strain	Titer ($g \cdot l^{-1}$)	Mw ($g \cdot mol^{-1}$)[a]	HPLC-MS recovery (%)[b]
WT	2.91 ± 0.09	$(8.93 \pm 1.56) \times 10^6$	55.1 ± 2.2
Δ*pepF*	1.74 ± 0.02	$(1.95 \pm 0.09) \times 10^7$	50.5 ± 2.5
Δ*pepJ*	1.31 ± 0.01	$(7.87 \pm 0.36) \times 10^6$	47.6 ± 2.8
Δ*pepC*	0.53 ± 0.06	$(1.70 \pm 0.05) \times 10^7$	46.2 ± 2.8
Δ*ugdH1*	0.53 ± 0.05	$(1.85 \pm 0.14) \times 10^7$	34.9 ± 1.7
Δ*manC*	No precipitate	$(1.56 \pm 0.15) \times 10^7$	Not measured

[a]Peak integration of the refractive index (RI) signal for molecular weight determinations was performed if the light scattering signal indicated presence of a polymer.
[b]Recoveries in HPLC-MS are reported as the sum of all quantifiable sugars relative to titer.

To compare sugar monomer compositions of produced WT and mutant EPSs, dried and ground polymer was re-dissolved, hydrolyzed and analyzed via HT-PMP analysis. The HPLC-MS data shows that all obtained polymers were composed of the same sugar monomers: glucose (Glc), mannose (Man), galactose (Gal), fucose (Fuc) and glucuronic acid (GlcA) (Figure 7). We assume that traces of glucosamine (GlcN) found in the samples are probably impurities from cell debris since its low amount does not suggest a stoichiometrically plausible participation in a conserved repeating unit. Sugar recoveries of about 50% during HPLC-MS (Table 3) are in the expected range for crude EPS batches (78). Since different sugars show different susceptibilities to release and degradation during hydrolysis, some are underrepresented in the final data.

Uronic acids, for example, are prone to degradation and can only be recovered partially (79). In contrast to this, dimers of uronic acids and hexoses are fairly stable, resulting in a reduced release and thereby reduced detection of attached hexose (78). Salts, co-precipitated protein and water, attracted by the hygroscopic EPS powders also contribute to recoveries below 100%. The compositions of Δ*pepC* and Δ*ugdH1* EPSs only displayed minor differences compared to the WT polymer, indicating that the produced EPSs are highly similar in monomer pattern. We assume that the enzymes encoded by *pepC* and *ugdH1* are crucial for EPS production, but that their functions are present twice in the clusters. Deletion of one copy might partially be taken over by its paralog, resulting in lower amounts but structurally identical EPS. *UgdH1* has a 64% protein sequence identity to *ugdH2*, and both genes were confidently annotated to catalyze the oxidation of UDP-Glc to UDP-GlcA. Hence, it is likely that knockout of only one *ugdH* gene does not completely eliminate synthesis of this component. A similar explanation accounts for the results of *pepC*, which exhibits a protein sequence identity of 60% with *pepQ* (Supplementary Figure S7). Multiple sequence alignment of all *P. polymyxa* GTs with priming GTs of *Streptococcus agalactiae* (CpsE) and *Lactobacillus helveticus* (EpsE) revealed that protein similarities of PepC and PepQ with EpsE and CpsE are above 40%, whereas the homologies of all other GTs with the annotated, priming GTs are below 22%. We therefore assume that *pepC* and *pepQ* encode two redundant priming glycosyl transferases.

The most interesting deletion mutants in terms of EPS structure are Δ*pepF* and Δ*pepJ*. These variants produced polymers with a significantly altered monomer distribution compared to the WT. In the case of Δ*pepJ*, the amount of mannose in the polymer was reduced by 15% and the amount of glucose by 7.5%, making galactose and fucose fill a correspondingly larger proportion of the overall composition.

In the case of the Δ*pepF* mutant, the galactose content is reduced to 50% of its WT content, accompanied by a near complete loss of pyruvate. This data suggests that 50% of the contained galactose molecules, are being pyruvylated, and that the pyruvate-substituted galactose monomer is transferred by *pepF*. The pyruvate group is typically added before secretion (80).

Since colony morphology and viscosity of liquid cultures indicated that the polymer produced by the Δ*pepF* mutant exhibited considerably different physicochemical characteristics than the WT, a comparison of the rheological behavior of WT and Δ*pepF* mutant EPS was performed. The results obtained by recording viscosity curves, amplitude sweeps and frequency sweeps clearly underscore the fundamental physicochemical differences between WT and Δ*pepF* polymer (Figure 8).

Although both EPSs create highly viscous, shear-thinning solutions when dissolved in water, their behavior upon stress and time is substantially different, making each interesting for entirely different applications. The WT EPS forms a gel-like

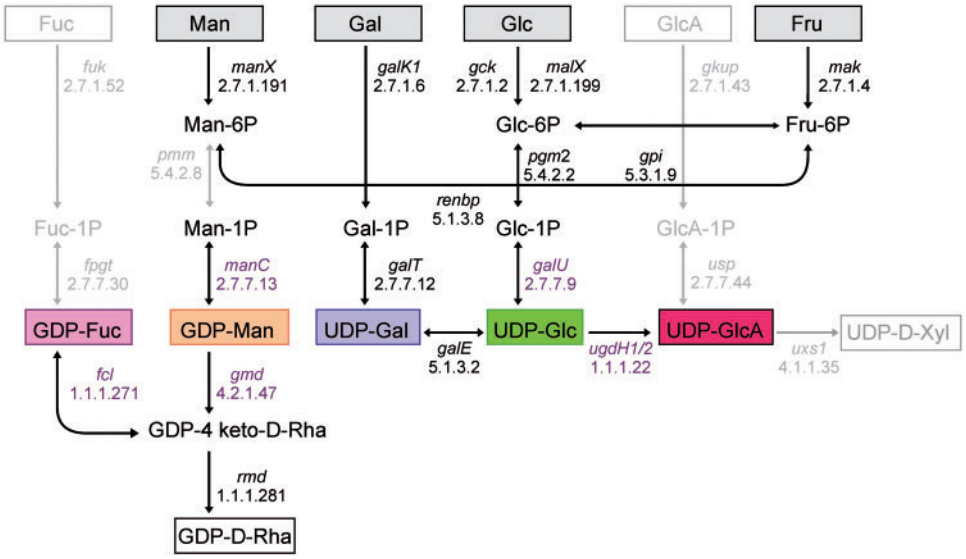

Figure 6. Biosynthetic pathways dedicated to the production of activated nucleotide sugars in *P. polymyxa*. The map was constructed based on a metabolic network model of a *P. polymyxa* strain annotated on KEGG database. All pathways present in the *P. polymyxa* genome are shown in black. Grey routes are not annotated. Enzymes written in purple are located within the EPS cluster, black ones somewhere else in the genome. Nucleotide sugars highlighted with color are constituents of the WT polymer.

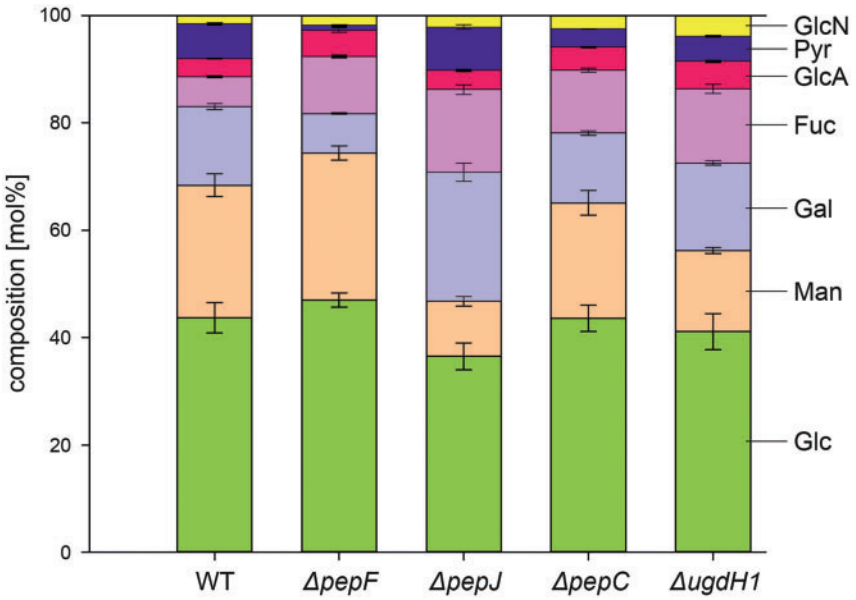

Figure 7. Sugar monomer compositions of EPSs from mutants and WT *P. polymyxa*. Pyruvate content was determined with a pyruvate oxidase assay. All other components were analyzed and quantified via HPLC-ESI-MS/MS.

structure with a pronounced network, delivering high viscosity and stability to mechanical stress. No viscosity plateau at low shear rates can be observed in the viscosity curves of the WT EPS, indicating that polymer strands are linked with each other via inter-molecular forces. The remarkable difference between G′ and G″ in amplitude sweeps describes the elastic character of the WT solution. Upon increase of applied strain, the degeneration of the sample network begins with a G″ overshoot, which probably occurs due to micro crack formation within the structured gel (81). The depicted frequency test points out the stability of the sample over time. Even at low frequencies, simulating long-term stress, the sample character remains dominated by the elastic modulus and does not show any tendencies to start flowing. The WT EPS could potentially be applied as stabilizer for suspensions or as hydrogel for biomedical, cosmetic or food applications. The generated mutant EPS, however, reveals remarkably different attributes. A distinct viscosity plateau can be observed in the flow curves, assigning this sample to the group of entangled polymers without a strong physicochemical network. At low shearing, polymer strands simultaneously ravel and unravel, resulting in constant friction (82). Similar contributions of elasticity and viscosity to the sample structure and the lack of a G″ overshoot in strain sweeps emphasize the viscous but not gel-like character of the mutant EPS. In frequency

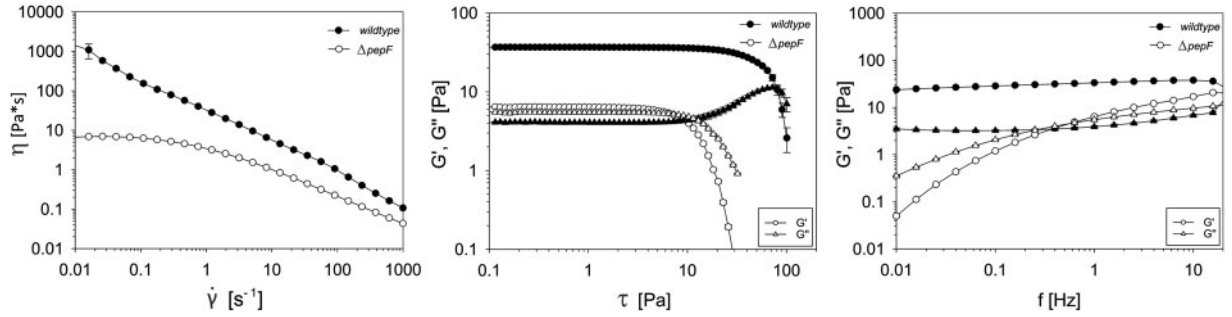

Figure 8. Rheological characterization of polymer produced by the WT and Δ*pepF* mutant. Viscosity curves (left), strain sweeps (middle) and frequency sweeps (right) of 1% EPS solutions in ultra-pure water were recorded on a controlled shear stress rheometer using a cone-plate geometry.

sweeps, this solution behaves like a typical Maxwell material. Sudden deformations, simulated by high frequencies, result in a rather elastic response of the material, whereas long-term stress induces viscous flowing of the solution. This polymer is suited for any application in which a shear thinning, viscous thickener is needed. Examples are cosmetic lotions, oil drilling fluids or paints and lacquers.

4. Conclusion

In the present study, we designed and adapted a CRISPR-Cas9 based genome-editing tool for *P. polymyxa* for the first time. We proved its functionality in knockout studies of single genes and large regions via sgRNA multiplexing and harnessed it for genome integration experiments. After implementation, we utilized the system to study the yet undescribed EPS biosynthesis machinery of *P. polymyxa*. Results obtained here yield the first insights into basic principles of this Wzx/Wzy pathway, and putative roles of selected key genes were assigned. Furthermore, we exemplified EPS tailoring through genetic recoding. Specifically, we generated mutant EPSs with significantly altered monomer compositions. Rheological characterization revealed that one of these polymer variants exhibits fundamentally different physicochemical properties than the WT, making it suitable for an entirely different set of applications. Future work will focus on the in-depth characterization of all genes involved in biosynthesis of *P. polymyxa* EPS in order to construct a biotechnologically relevant production strain for tailor-made EPS. Thorough chemical structure analysis via NMR will enhance our understanding of structure–function relationships of generated EPS variants. Furthermore, an already constructed, inactivated variant of the pCasPP plasmid (pdCasPP) will be used for CRISPRi-mediated repression studies in *P. polymxa*. We also anticipate that the vector system will expedite research in distinct fields related to *Paenibacilli*, including the production of other value-added products like 2,3-butanediol and health related issues like *P. larvae* pathogenesis in honeybee larvae.

Supplementary data

Supplementary Data are available at *SYNBIO* Online.

Acknowledgements

Special thanks go to José Guillermo Ortiz Tena for technical and scientific support in analytical measurements.

Funding

Evonik Industries; DECHEMA (in part).

Conflict of interest statement. None declared.

References

1. Du,J., Shao,Z. and Zhao,H. (2011) Engineering microbial factories for synthesis of value-added products. *J. Ind. Microbiol. Biotechnol.*, 38, 873–890.
2. Rehm,B.H. (2010) Bacterial polymers: biosynthesis, modifications and applications. *Nat. Rev. Microbiol.*, 8, 578–592.
3. Bhan,N., Xu,P. and Koffas,M.A.G. (2013) Pathway and protein engineering approaches to produce novel and commodity small molecules. *Curr. Opin. Biotechnol.*, 24, 1137–1143.
4. Wenzel,S.C. and Müller,R. (2005) Recent developments towards the heterologous expression of complex bacterial natural product biosynthetic pathways. *Curr. Opin. Biotechnol.*, 16, 594–606.
5. Cress,B.F., Trantas,E.A., Ververidis,F., Linhardt,R.J. and Koffas,M.A.G. (2015) Sensitive cells: enabling tools for static and dynamic control of microbial metabolic pathways. *Curr. Opin. Biotechnol.*, 36, 205–214.
6. Mougiakos,I., Bosma,E.F., de Vos,W.M., van Kranenburg,R. and van der Oost,J. (2016) Next generation prokaryotic engineering: the CRISPR-Cas toolkit. *Trends Biotechnol.*, 34, 575–587.
7. Chow,V., Kim,Y.S., Rhee,M.S., Sawhney,N., St John,F.J., Nong,G., Rice,J.D. and Preston,J.F. (2016) A 1, 3-1, 4-β-glucan utilization regulon in *Paenibacillus* sp. strain JDR-2. *Appl. Environ. Microbiol.*, 82, 1789–1798.
8. Sharmin,F., Wakelin,S., Huygens,F. and Hargreaves,M. (2013) Firmicutes dominate the bacterial taxa within sugar-cane processing plants. *Sci. Rep.*, 3, 3107.
9. Devaraj,S., Hemarajata,P. and Versalovic,J. (2013) The human gut microbiome and body metabolism: implications for obesity and diabetes. *Clin. Chem.*, 59, 617–628.
10. Aleti,G., Sessitsch,A. and Brader,G. (2015) Genome mining: prediction of lipopeptides and polyketides from Bacillus and related Firmicutes. *Comp. Struct. Biotechnol. J.*, 13, 192–203.
11. Ju,F., Guo,F., Ye,L., Xia,Y. and Zhang,T. (2014) Metagenomic analysis on seasonal microbial variations of activated sludge from a full-scale wastewater treatment plant over 4 years. *Environ. Microbiol. Rep.*, 6, 80–89.
12. Giraffa,G., Chanishvili,N. and Widyastuti,Y. (2010) Importance of lactobacilli in food and feed biotechnology. *Res. Microbiol.*, 161, 480–487.
13. Jones,D.T. and Woods,D.R. (1986) Acetone-butanol fermentation revisited. *Microbiol. Rev.*, 50, 484–524.

14. Altenbuchner,J. (2016) Editing of the *Bacillus subtilis* genome by the CRISPR-Cas9 system. *Appl. Environ. Microbiol.*, 82, 5421–5427.
15. Zhang,K., Duan,X. and Wu,J. (2016) Multigene disruption in undomesticated *Bacillus subtilis* ATCC 6051a using the CRISPR/Cas9 system. *Sci. Rep.*, 6, 27943.
16. Westbrook,A.W., Moo-Young,M. and Chou,C.P. (2016) Development of a CRISPR-Cas9 toolkit for comprehensive engineering of *Bacillus subtilis*. *Appl. Environ. Microbiol.*, 82, 4876–4895.
17. Oh,J.-H. and van Pijkeren,J.-P. (2014) CRISPR–Cas9-assisted recombineering in *Lactobacillus reuteri*. *Nucleic Acids Res.*, 42, e131.
18. Pyne,M.E., Bruder,M.R., Moo-Young,M., Chung,D.A. and Chou,C.P. (2016) Harnessing heterologous and endogenous CRISPR-Cas machineries for efficient markerless genome editing in *Clostridium*. *Sci. Rep.*, 6, 25666.
19. Chen,W., Zhang,Y., Yeo,W.-S., Bae,T. and Ji,Q. (2017) Rapid and efficient genome editing in *Staphylococcus aureus* by using an engineered CRISPR/Cas9 system. *J. Am. Chem. Soc.*, 139, 3790–3795.
20. Kim,S-B. and Timmusk,S. (2013) A simplified method for gene knockout and direct screening of recombinant clones for application in *Paenibacillus polymyxa*. *PLoS One*, 8, e68092.
21. Zarschler,K., Janesch,B., Zayni,S., Schäffer,C. and Messner,P. (2009) Construction of a gene knockout system for application in *Paenibacillus alvei* CCM 2051T, exemplified by the S-layer glycan biosynthesis initiation enzyme WsfP. *Appl. Environ. Microbiol.*, 75, 3077–3085.
22. Genersch,E. (2010) American Foulbrood in honeybees and its causative agent, *Paenibacillus larvae*. *J. Invertebr. Pathol.*, 103(Suppl.1), S10–S19.
23. Padhi,S., Dash,M., Sahu,R. and Panda,P. (2013) Urinary tract infection due to *Paenibacillus alvei* in a chronic kidney disease: a rare case report. *J. Lab. Physicians*, 5, 133–135.
24. Roux,V., Fenner,L. and Raoult,D. (2008) *Paenibacillus provencensis* sp. nov., isolated from human cerebrospinal fluid, and *Paenibacillus urinalis* sp. nov., isolated from human urine. *Int. J. Syst. Evol. Microbiol.*, 58, 682–687.
25. Xie,J-B., Du,Z., Bai,L., Tian,C., Zhang,Y., Xie,J-Y., Wang,T., Liu,X., Chen,X. and Cheng,Q. (2014) Comparative genomic analysis of N_2 fixing and non-N_2-fixing *Paenibacillus* spp.: organization, evolution and expression of the nitrogen fixation genes. *PLoS Genet.*, 10, e1004231.
26. Xie,J., Shi,H., Du,Z., Wang,T., Liu,X. and Chen,S. (2016) Comparative genomic and functional analysis reveal conservation of plant growth promoting traits in *Paenibacillus polymyxa* and its closely related species. *Sci. Rep.*, 6, 21329.
27. Klein,M.G. (1988) Pest management of soil-inhabiting insects with microorganisms. *Agric. Ecosyst. Environ.*, 24, 337–349.
28. Storm,D.R., Rosenthal,K.S. and Swanson,P.E. (1977) Polymyxin and related peptide antibiotics. *Annu. Rev. Biochem.*, 46, 723–763.
29. Kajimura,Y., Kaneda,M. and Fusaricidin,A. (1996) a New depsipeptide antibiotic produced by *Bacillus polymyxa* KT-8. *J. Antibiot.*, 49, 129–135.
30. Häßler,T., Schieder,D., Pfaller,R., Faulstich,M. and Sieber,V. (2012) Enhanced fed-batch fermentation of 2,3-butanediol by *Paenibacillus polymyxa* DSM 365. *Bioresour. Technol.*, 124, 237–244.
31. Rütering,M., Schmid,J., Rühmann,B., Schilling,M. and Sieber,V. (2016) Controlled production of polysaccharides–exploiting nutrient supply for levan and heteropolysaccharide formation in *Paenibacillus* sp. *Carbohydr. Polym.*, 148, 326–334.
32. Raza,W., Makeen,K., Wang,Y., Xu,Y. and Qirong,S. (2011) Optimization, purification, characterization and antioxidant activity of an extracellular polysaccharide produced by *Paenibacillus polymyxa* SQR-21. *Bioresour. Technol.*, 102, 6095–6103.
33. Kim,S-W., Ahn,S-G., Seo,W-T., Kwon,G-S. and Park,Y-H. (1998) Rheological properties of a novel high viscosity polysaccharide, A49-Pol, produced by *Bacillus polymyxa*. *J. Microbiol. Biotechnol.*, 8, 178–181.
34. Liang,T-W. and Wang,S-L. (2015) Recent advances in exopolysaccharides from *Paenibacillus* spp.: production, isolation, structure, and bioactivities. *Mar. Drugs*, 13, 1847–1863.
35. Kahng,G-G., Lim,S-H., Yun,H-D. and Seo,W-T. (2001) Production of extracellular polysaccharide, EPS WN9, from *Paenibacillus* sp. WN9 KCTC 8951P and its usefulness as a cement mortar admixture. *Biotechnol. Bioprocess Eng.*, 6, 112–116.
36. Grady,E.N., MacDonald,J., Liu,L., Richman,A. and Yuan,Z.-C. (2016) Current knowledge and perspectives of Paenibacillus: a review. *Microb. Cell Fact.*, 15, 203.
37. Schmid,J., Sieber,V. and Rehm,B. (2015) Bacterial exopolysaccharides: biosynthesis pathways and engineering strategies. *Front. Microbiol.*, 6, 496.
38. Toukach,P.V. (2011) Bacterial carbohydrate structure database 3: principles and realization. *J. Chem. Inf. Model*, 51, 159–170.
39. Freitas,F., Alves,V.D. and Reis,M.A. (2011) Advances in bacterial exopolysaccharides: from production to biotechnological applications. *Trends Biotechnol.*, 29, 388–398.
40. Schmid,J., Sperl,N. and Sieber,V. (2014) A comparison of genes involved in sphingan biosynthesis brought up to date. *Appl. Microbiol. Biotechnol.*, 98, 7719–7733.
41. Freitas,F., Alves,V. and Reis,M.M. (2014) Bacterial polysaccharides: production and applications in cosmetic industry. In: R Kishan Gopal and M Jean-Michel (eds) *Polysaccharides*. Springer International Publishing, Cham, pp. 1–24.
42. Ates,O. (2015) Systems biology of microbial exopolysaccharides production. *Front. Bioeng. Biotechnol.*, 3, 200.
43. Rehm,B.H.A. (2015) Synthetic biology towards the synthesis of custom-made polysaccharides. *Microb. Biotechnol.*, 8, 19–20.
44. Becker,A. (2015) Challenges and perspectives in combinatorial assembly of novel exopolysaccharide biosynthesis pathways. *Front. Microbiol.*, 6, 687.
45. Hassler,R.A. and Doherty,D.H. (1990) Genetic engineering of polysaccharide structure: production of variants of xanthan gum in *Xanthomonas campestris*. *Biotechnol. Prog.*, 6, 182–187.
46. Welman,A.D. and Maddox,I.S. (2003) Exopolysaccharides from lactic acid bacteria: perspectives and challenges. *Trends Biotechnol.*, 21, 269–274.
47. Schmid,J. and Sieber,V. (2015) Enzymatic transformations involved in the biosynthesis of microbial exo-polysaccharides based on the assembly of repeat units. *ChemBioChem*, 16, 1141–1147.
48. ——, Heider,D., Wendel,N.J., Sperl,N. and Sieber,V. (2016) Bacterial glycosyltransferases: challenges and opportunities of a highly diverse enzyme class toward tailoring natural products. *Front. Microbiol.*, 7, 182.
49. Boe,L., Gros,M.F., Te Riele,H., Ehrlich,S.D. and Gruss,A. (1989) Replication origins of single-stranded-DNA plasmid pUB110. *J. Bacteriol.*, 171, 3366–3372.
50. Novotny,R., Novotny,R., Berger,H., Schinko,T., Messner,P., Schäffer,C. and Strauss,J. (2008) A temperature-sensitive expression system based on the Geobacillus stearothermophilus NRS 2004/3a sgsE surface-layer gene promoter. *Biotechnol. Appl. Biochem.*, 49, 35–40.
51. Aziz,R.K., Bartels,D., Best,A.A., DeJongh,M., Disz,T., Edwards,R.A., Formsma,K., Gerdes,S., Glass,E.M., Kubal,M.

et al. (2008) The RAST server: rapid annotations using subsystems technology. *BMC Genomics*, 9, 75.
52. Altschul,S.F., Gish,W., Miller,W., Myers,E.W. and Lipman,D.J. (1990) Basic local alignment search tool. *J. Mol. Biol.*, 215, 403–410.
53. Apweiler,R., Bairoch,A., Wu,C.H., Barker,W.C., Boeckmann,B., Ferro,S., Gasteiger,E., Huang,H., Lopez,R. and Magrane,M. *et al*. (2004) UniProt: the Universal Protein knowledgebase. *Nucleic Acids Res*, 32(suppl_1), D115–D119.
54. Yu,C-S., Lin,C-J. and Hwang,J-K. (2004) Predicting subcellular localization of proteins for Gram-negative bacteria by support vector machines based on n-peptide compositions. *Protein Sci.*, 13, 1402–1406.
55. Kanehisa,M. and Goto,S. (2000) KEGG: Kyoto encyclopedia of genes and genomes. *Nucleic Acids Res.*, 28, 27–30.
56. Cobb,R.E., Wang,Y. and Zhao,H. (2015) High-efficiency multiplex genome editing of streptomyces species using an engineered CRISPR/Cas system. *ACS Synth. Biol.*, 4, 723–728.
57. Rühmann,B., Schmid,J. and Sieber,V. (2014) Fast carbohydrate analysis via liquid chromatography coupled with ultra violet and electrospray ionization ion trap detection in 96-well format. *J. Chrom. A*, 1350, 44–50.
58. ——, —— and —— (2016) Automated modular high throughput exopolysaccharide screening platform coupled with highly sensitive carbohydrate fingerprint analysis. *J. Vis. Exp*. doi:10.3791/53249.
59. Müller,A.K., Rojo,F. and Alonso,J.C. (1995) The level of the pUB110 replication initiator protein is autoregulated, which provides an additional control for plasmid copy number. *Nucleic Acids Res.*, 23, 1894–1900.
60. Engler,C., Kandzia,R. and Marillonnet,S. (2008) A one pot, one step, precision cloning method with high throughput capability. *PLoS One*, 3, e3647.
61. Jiang,W., Bikard,D., Cox,D., Zhang,F. and Marraffini,L.A. (2013) RNA-guided editing of bacterial genomes using CRISPR-Cas systems. *Nat. Biotechnol.*, 31, 233–239.
62. Xie,N-Z., Li,J-X., Song,L-F., Hou,J-F., Guo,L., Du,Q-S., Yu,B. and Huang,R-B. (2015) Genome sequence of type strain *Paenibacillus polymyxa* DSM 365, a highly efficient producer of optically active (R, R)-2, 3-butanediol. *J. Biotechnol.*, 195, 72–73.
63. Whitfield,C. (2006) Biosynthesis and assembly of capsular polysaccharides in *Escherichia coli*. *Annu. Rev. Biochem.*, 75, 39–68.
64. Yother,J. (2011) Capsules of *Streptococcus pneumoniae* and other bacteria: paradigms for polysaccharide biosynthesis and regulation. *Annu. Rev. Microbiol.*, 65, 563–581.
65. Becker,A., Katzen,F., Pühler,A. and Ielpi,L. (1998) Xanthan gum biosynthesis and application: a biochemical/genetic perspective. *Appl. Microbiol. Biotechnol.*, 50, 145–152.
66. Jolly,L. and Stingele,F. (2001) Molecular organization and functionality of exopolysaccharide gene clusters in lactic acid bacteria. *Int. Dairy J.*, 11, 733–745.
67. Bezzate,S., Aymerich,S., Chambert,R., Czarnes,S., Berge,O. and Heulin,T. (2000) Disruption of the *Paenibacillus polymyxa* levansucrase gene impairs its ability to aggregate soil in the wheat rhizosphere. *Environ. Microbiol.*, 2, 333–342.
68. Jolly,L., Newell,J., Porcelli,I., Vincent,S.J.F. and Stingele,F. (2002) *Lactobacillus helveticus* glycosyltransferases: from genes to carbohydrate synthesis. *Glycobiology*, 12, 319–327.
69. Péant,B., LaPointe,G., Gilbert,C., Atlan,D., Ward,P. and Roy,D. (2005) Comparative analysis of the exopolysaccharide biosynthesis gene clusters from four strains of *Lactobacillus rhamnosus*. *Microbiology*, 151, 1839–1851.
70. Wu,Q., Tun,H.M., Leung,F.C-C. and Shah,N. P. (2014) Genomic insights into high exopolysaccharide-producing dairy starter bacterium *Streptococcus thermophilus* ASCC 1275. *Sci. Rep.*, 4, 4974.
71. Kim,S-Y., Kim,J-G., Lee,B-M. and Cho,J-Y. (2008) Mutational analysis of the gum gene cluster required for xanthan biosynthesis in *Xanthomonas oryzae* pv oryzae. *Biotechnol. Lett.*, 31, 265.
72. Cieslewicz,M.J., Kasper,D.L., Wang,Y. and Wessels,M.R. (2001) Functional analysis in type Ia Group B *Streptococcus* of a cluster of genes involved in extracellular polysaccharide production by diverse species of Streptococci. *J. Biol. Chem.*, 276, 139–146.
73. Lamothe,G., Jolly,L., Mollet,B. and Stingele,F. (2002) Genetic and biochemical characterization of exopolysaccharide biosynthesis by *Lactobacillus delbrueckii* subsp. bulgaricus. *Arch. Microbiol.*, 178, 218–228.
74. Boels,I.C., Kranenburg,R. v., Hugenholtz,J., Kleerebezem,M. and de Vos,W.M. (2001) Sugar catabolism and its impact on the biosynthesis and engineering of exopolysaccharide production in lactic acid bacteria. *Int. Dairy J.*, 11, 723–732.
75. Li,O., Qian,C-D., Zheng,D-Q., Wang,P-M., Liu,Y., Jiang,X-H. and Wu,X-C. (2015) Two UDP-glucuronic acid decarboxylases involved in the biosynthesis of a bacterial exopolysaccharide in *Paenibacillus elgii*. *Appl. Microbiol. Biotechnol.*, 99, 3127–3139.
76. Weon-Taek,S., Kahng,G-G., Nam,S-H., Choi,S-D., Suh,H-H., Kim,S-W. and Park,Y-H. (1999) Isolation and characterization of a novel exopolysaccharide-producing *Paenibacillus* sp. WN9 KCTC 8951P. *J. Microbiol. Biotechnol.*, 9, 820–825.
77. Cole,J.N., Aziz,R.K., Kuipers,K., Timmer,A.M., Nizet,V. and van Sorge,N.M. (2012) A conserved UDP-glucose dehydrogenase encoded outside the hasABC operon contributes to capsule biogenesis in Group A Streptococcus. *J. Bacteriol.*, 194, 6154–6161.
78. Rühmann,B., Schmid,J. and Sieber,V. (2015) High throughput exopolysaccharide screening platform: from strain cultivation to monosaccharide composition and carbohydrate fingerprinting in one day. *Carbohydr. Polym.*, 122, 212–220.
79. Tait,M.I., Sutherland,I.W. and Clarke-Sturman,A.J. (1990) Acid hydrolysis and high-performance liquid chromatography of xanthan. *Carbohydr. Polym.*, 13, 133–148.
80. Katzen,F., Ferreiro,D.U., Oddo,C.G., Ielmini,M.V., Becker,A., Pühler,A. and Ielpi,L. (1998) *Xanthomonas campestris* pv. campestrisgum mutants: effects on xanthan biosynthesis and plant virulence. *J. Bacteriol.*, 180, 1607–1617.
81. Hyun,K., Wilhelm,M., Klein,C.O., Cho,K-S., Nam,J-G., Ahn,K-H., Lee,S-J., Ewoldt,R.H. and McKinley,G.H. (2011) A review of nonlinear oscillatory shear tests: analysis and application of large amplitude oscillatory shear (LAOS). *Prog. Polym. Sci.*, 36, 1697–1753.
82. Graessley,W.W. (1967) Viscosity of entangling polydisperse polymers. *J. Chem. Phys.*, 47, 1942–1953.